

Multicasting Optical Reconfigurable Switch

Niyazi Ulas Dinc^{1, †}, Mustafa Yildirim^{1, †}, Christophe Moser¹, and Demetri Psaltis²

¹ Laboratory of Applied Photonics Devices, Ecole Polytechnique Fédérale de Lausanne (EPFL), Switzerland

² Ecole Polytechnique Fédérale de Lausanne (EPFL), Switzerland

† Equally contributing authors.

Abstract

Artificial Intelligence (AI) demands large data flows within datacenters, heavily relying on multicasting data transfers. As AI models scale, the requirement for high-bandwidth and low-latency networking compounds. The common use of electrical packet switching faces limitations due to its optical-electrical-optical conversion bottleneck. Optical switches, while bandwidth-agnostic and low-latency, suffer from having only unicast or non-scalable multicasting capability. This paper introduces an optical switching technique addressing the scalable multicasting challenge. Our approach enables arbitrarily programmable simultaneous unicast and multicast connectivity, eliminating the need for optical splitters that hinder scalability due to optical power loss. We use phase modulation in multiple planes, tailored to implement any multicast connectivity map. Using phase modulation enables wavelength selectivity on top of spatial selectivity, resulting in an optical switch that implements space-wavelength routing. We conducted simulations and experiments to validate our approach. Our results affirm the concept's feasibility and effectiveness, as a multicasting switch.

Datacenters manage and process large volumes of data, comprising thousands of computing nodes alongside networking and storage systems. The networking fabric enables interconnection across many devices to execute workloads efficiently. Traditionally, data routing within a datacenter relied on electrical packet switching through fiber optic cables, where an electronic switch receives a data packet, processes, and regenerates it for the target port. On the other hand, optical circuit switches (OCS) directly route the incoming light to the target port. While the packet reading of the electrical switch allows message replication or extra processing in the switch, they are not possible with OCS. Meanwhile, network management has evolved, and software-defined networking (SDN) has been established to manage the datacenter network more efficiently, optimizing global traffic across the entire datacenter [1]. In traditional network architectures, network devices by themselves make decisions about where to forward data, based on pre-defined protocols. SDN, on the other hand, separates the control plane (deciding where traffic should be sent) from the data plane (the actual forwarding of the traffic). Therefore, it is not necessary anymore to read packets, instead, the centralized controller can communicate the connectivity map to the switch. This evolution already enabled the adaptation of unicast (one-to-one) OCS in datacenters [2-4].

Large AI models can easily occupy thousands of compute nodes, where model parameters and dataset are multicasted among nodes iteratively during training [5, 6]. As the volume of multicast communication patterns increases alongside the scale of operations, network congestion becomes unavoidable due to the excess use of bandwidths. Current optical switches cater solely to unicast, managing multicast via message replication with tandem use of electronic switches or passive power splitters coupled with programmable unicasting OCSes [4, 6-9]. However, the latter's power loss (due to many fixed divisions) curbs scalability, leaving a need for scalable and reconfigurable OCS's equipped with both unicast and multicast functionalities.

Optical circuit switches based on microelectromechanical systems (MEMS) mirrors [10] is a deployed optical interconnect technology. While MEMS switches can provide energy-efficient optical routing, they cannot multicast single input to many output channels. This arises from the ray-optic characteristics when using millimeter-sized, two-axis continuously rotating mirrors or the binary modulation characteristics when

utilizing digital Micromirror devices. Moreover, the former systems are not wavelength sensitive, only satisfying space granularity [3, 4]. Another solution, Wavelength-selective switches (WSSs) are devices capable of redirecting optical signals to different output ports based on their wavelengths. These switches typically consist of a one-dimensional (1D) diffraction grating and a beam-steering mechanism. The diffraction grating disperses the optical signals into their constituent wavelengths, while the beam-steering mechanism directs them to specific output ports based on their wavelengths. In many WSSs, Liquid-Crystal-on-Silicon (LCoS) spatial light modulators are utilized as beam-steering devices [11, 12]. However, a limitation of WSSs is that they can only redirect one input signal to one output port at a time. Consequently, WSSs are also unsuitable for multicasting. Moreover, 1D input/output configuration also hampers the scalability of WSSs unless it is combined by MEMS-based re-routing at the cost of increased complexity [12]. Contrarily, fixed interconnect methodologies, such as printed diffractive layers [13, 14], waveguides [15], and volume holograms [16, 17] are studied to address some of the mentioned challenges. However, they are non-programmable, restricting their applicability in dynamic environments like datacenters.

In this work, we present a multicasting optical reconfigurable switch (MORS) capable of multicast and wavelength selectivity. Our method leverages spatial light modulation on multiple planes to enable on-demand reconfiguration of optical paths consisting of both unicast and multicast connections (Fig. 1a). The schematic diagram of MORS is shown in Fig. 1b. Input beams traverse the multiple modulation planes, while wavefront shaping arranges the optical paths corresponding to each input. The physical realization of MORS combines a liquid crystal Spatial Light Modulator (SLM) with a folding mirror positioned across the SLM display. This arrangement permits the concurrent display of multiple modulation planes on a single SLM device, creating a multi-bounce single-pass cavity as depicted in Figures 1c and 1d. Within this setup, each plane acts as a thin modulating element, altering the phase of the light as it propagates between planes. In Fig. 1c, the spatial-only (broadband response in wavelength) interconnect is illustrated, where different inputs experience unicast and multicast scenarios, respectively. In Fig. 1d, we show unicast and multicast for wavelength channels entering from the same input position/space. In this configuration, the channels are mapped to distinct spatial positions based on their

respective wavelengths as desired. Fig. 1e displays a photograph of our optical cavity.

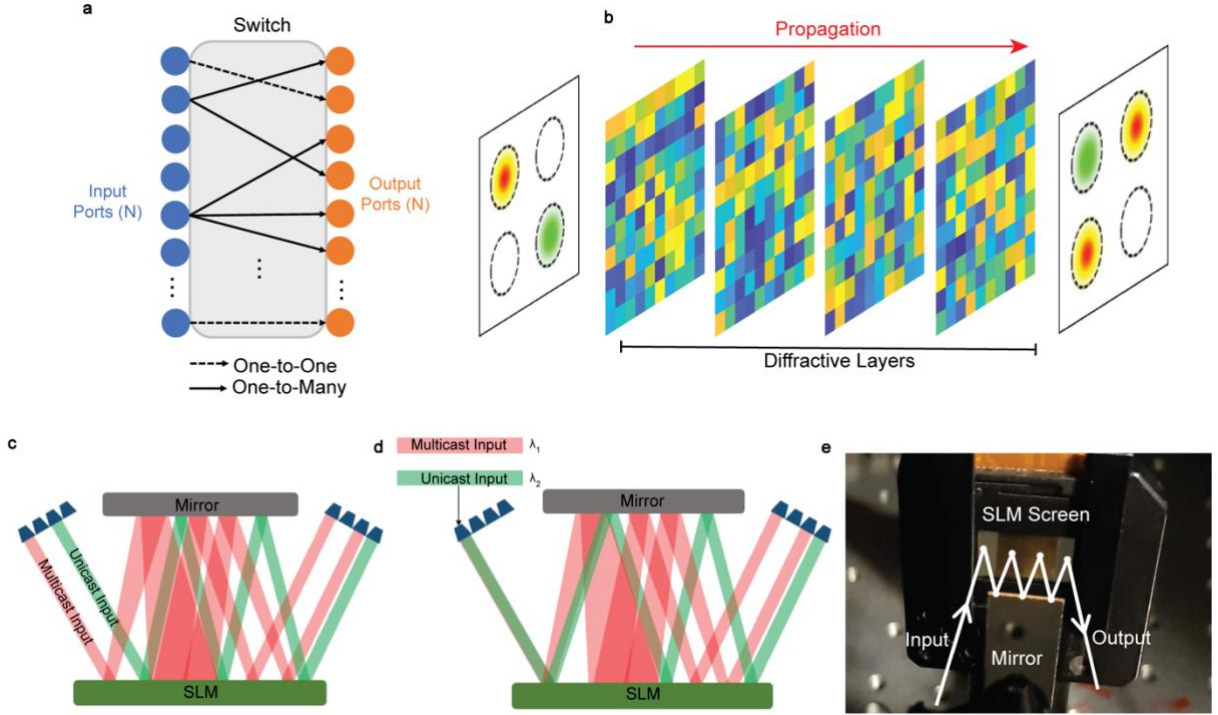


Figure 1: implementation of MORS. a) Schematic representation of an optical switch capable of several concurrent unicast (One-to-One) and multicast (One-to-Many) connections. b) Conceptual implementation of MORS consisting of wavefront modulation over multiple planes where the input plane on left-hand side show two incoming light beams that are routed to different ports at the output plane with specific examples of unicast (One-to-One) and multicast (One-to-Two) connections. c) Schematic representation of the physical implementation with an SLM display and a mirror across to use multiple planes (patches on a single SLM display) showcasing unicast and multicast connectivity like sub-Figure b. d) Example of wavelength selective unicast and multicast connections. e) Laboratory realization of MORS using four modulation planes on a single SLM display.

Results

The MORS technique is based on using multiple evenly spaced phase-only modulation planes. The Beam Propagation Method (BPM) helps determine the phase patterns displayed on the SLM, serving as the forward model in our optimization. We utilize an error backpropagation routine thanks to having a differentiable forward model [18-20], which we refer to as Learning Tomography in our previous studies [14, 21, 22], optimizing the input as ports that produce the incidence beam and desired outputs as the target outputs. To achieve spectral selectivity, we execute the forward model for each wavelength, adjusting the pixel phase based on the aggregated backpropagated error signals. For our tests, a tunable continuous wave laser is employed where an SLM and mirror created the multi-bounce, single pass cavity with four modulation

layers. To channel the beam to the first modulation layer on SLM, 4F imaging is used, relaying the beam that is reflected off a digital micromirror device (DMD). This DMD acts to emulate the input grid by activating specific sub-regions. Following the last reflection, the beam is relayed to a CMOS camera with a second 4F system. Refer to the Methods section for further details.

Multicast

On-demand multicast is defined as splitting the data carrying light beam based on the number of destination ports and routing them to these ports (see Fig. 2a). We use the term “on-demand” to refer to the fact that the number of destinations and their positions can be changed arbitrarily. The current approach in industry for on-demand multicast employs fixed power splitters to with optical unicast switches, where the fixed splitter divide the light from each input port to a pre-defined output port count. An optical unicast switch, like MEMS-based mirror arrays, acts as a shutter to control light passage. In this approach, a switch with N input/output ports splits each input light into N paths, regardless of the demanded multicast port count (N_m). When the number of multicast receivers is less than the output ports ($N_m < N$), power to non-receiving ($N - N_m$) output ports is wasted, impacting power efficiency (utilized output power divided by input power). Hence such devices are typically limited to 16 output ports. However, this is a very small number considering that unicast switches can employ up to a few hundred ports [23]. In Fig. 2b we show how the efficiency is severely hampered if one constructs a multicast switch based on ideal fixed splitters as the number of output ports (N) scales. Such a system is only 100% efficient when all the output ports receive data ($N_m = N$) as shown in Fig. 2e. On the other hand, a switch capable of performing on-demand multicast ideally should be lossless as shown in Fig. 2c, where the incoming power from each input port is split just by the number of required multicast output ports, N_m . MORS accounts each connectivity map separately and generates respective phase patterns. Therefore, input light is actively divided with respect to the demanded N_m rather being set to N as in fixed splitters.

We conducted a numerical scaling study of MORS by varying the port count (N) across a range from 4 to 128 for various multicast port counts (N_m). The outcomes are presented in Fig. 2d. In comparison to a passive splitter, our observations reveal that

MORS's power efficiency consistently surpasses that of the passive splitter in the regime where $N_m < N$. Notably, the efficiency declines as N_m increases, except for the case where N equals N_m . This decline is attributed to the difficulties associated with reconfiguring the switch with a fixed number of degrees of freedom. In cases where N equals N_m , only one input port can be active at a time. Conversely, when N_m is less than N , more than one input is active, leading to the sharing of free parameters among different inputs. Consequently, a higher number of multicasting ports necessitates more parameters, resulting in reduced power efficiency for such ports. We performed a real optical experiment for N up to 16 and its efficiencies are plotted in Fig. 2g. The experiments demonstrate a similar trend as the simulations.

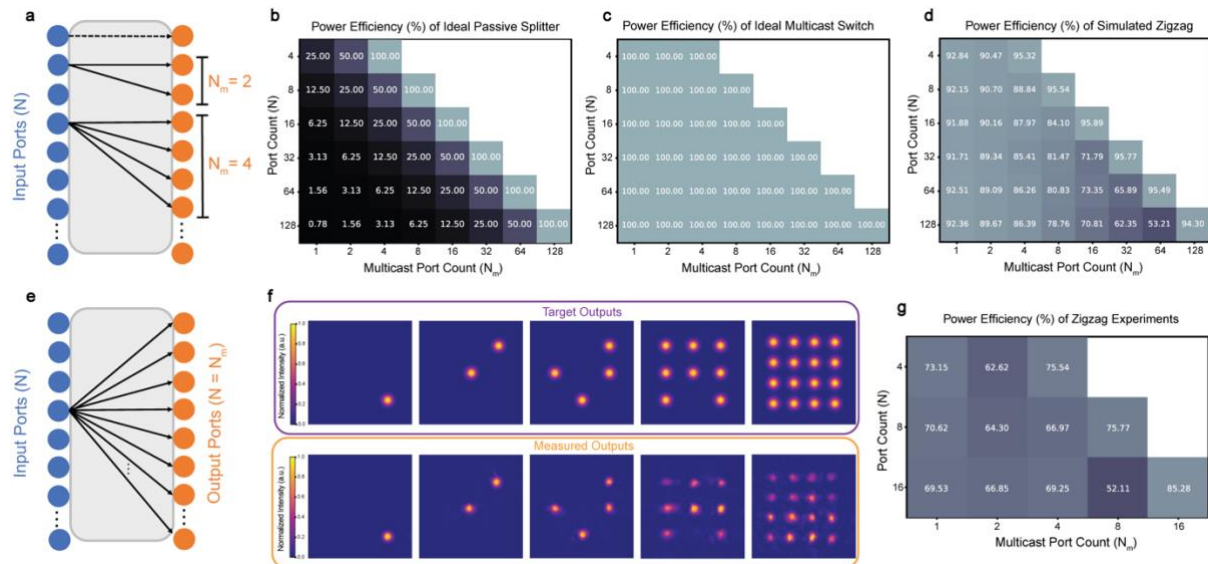


Figure 2: description and comparison of fixed multicast and on-demand multicast along with numerical and experimental efficiency results of MORS. a) Sketch of a switch that performs on-demand multicast and unicast where the number of multicast connections is less than the number of output ports b) Scaling of power efficiency of an ideal passive splitter with respect to the number of output ports (N) and utilized output ports (N_m) for multicast connections. c) On-demand multicast switch scales without loss ideally. d) The numerical results for scaling of MORS with finite degrees of freedom. e) Sketch of a switch where one input broadcasts its signal to all the output ports ($N_m = N$). f) Examples of experimental results obtained with MORS for on-demand multicast, given with corresponding target power distributions in the output plane. g) Experimental results for scaling of MORS that include the effects of finite degrees of freedom and experimental imperfections carried out up to $N=16$.

Space-Wavelength Granularity

Wavelength division multiplexing is a technique used in communication networks to enhance the capacity of spatial channels by aggregating signals with distinct wavelengths onto a shared channel. WSS functions by initially dispersing an incoming

beam based on wavelength and subsequently directing each wavelength channel to its target port. So, one can extend spatial switch to accommodate spectral switching by simply combining both. While it is plausible to extend a spatial switch to encompass spectral switching by combining both, such an approach introduces more complexity and diminished energy efficiency. Since light diffraction depends on wavelength, MORS can execute both space and wavelength simultaneously without any additional WSS layer. Moreover, iterative calculation of MORS handles seamlessly 2D input and output grids, which is a major improvement for scalability compared to WSS as they operate on 1D input and output grids.

There are two possible switching scenarios: either all wavelengths have the same connectivity map (i.e. broadband response) or all arbitrarily chosen (i.e. wavelength-selective response). We can achieve wavelength-selective connections by performing aggregated simulations where we run the forward model for each wavelength. After the optimization step, we can also probe the wavelength response numerically by running the forward model for many wavelength steps spanning the values that are used in the optimization, which we will refer to as “training wavelength”. For a pedagogical flow, we start with using a single training wavelength (850 nm) for a switch that has $N=4$ input and $N=4$ output nodes. We summarize the performance using an efficiency-crosstalk plot that is a similar representation to a transmission matrix where we place the correctly routed powers on the diagonal and off-diagonal values show the crosstalk as depicted in Fig. 3a where the values represent the mean of 10 randomly chosen connectivity maps numerically calculated resulting in -0.22 dB mean insertion loss and -30.71 dB mean crosstalk. In Fig 3d, we show the wavelength response of this device, which is relatively broadband spanning roughly 200 nm range with efficiency staying above 50%. When we use five training wavelengths as indicated in the plot in Fig. 3d, and set the connectivity maps the same for all the training wavelengths, we see that we can make the response even more flat with a few percent efficiency drop in the central wavelength as a trade-off. Then, for the wavelength-sensitive design, we keep the spatial port numbers the same but assign four training wavelength channels that are 30 nm apart where each wavelength has an arbitrarily different connectivity map. In this case, we have four efficiency-crosstalk plots for each wavelength channel. We plot them on a bigger matrix, which gives an overview of allowed conversions among spatial and wavelength channels. The non-filled off-

diagonal parts are not allowed since there is no mechanism to carry out frequency conversion. This representation is provided in Fig. 3b, where the mean insertion loss among 10 randomly chosen connectivity maps becomes -0.59 dB, and the mean crosstalk becomes -20.22 dB. In Fig. 3e, we provide the wavelength response for a specific connectivity map where the spatial output ports do not overlap for ease of representation of the individual wavelength channels. From Fig. 3e we see that there is a huge bandwidth allocation for the chosen wavelength channels considering that 1 nm corresponds to >400 GHz at 850 nm central wavelength. For the experiments, we show the wavelength selectivity for two wavelengths at 835 nm and 865 nm and provide the experimentally obtained efficiency-crosstalk plot in Fig. 3c. In these experiments, we obtained -2.10 dB insertion loss and -19.12 dB crosstalk over ten random connectivity maps.

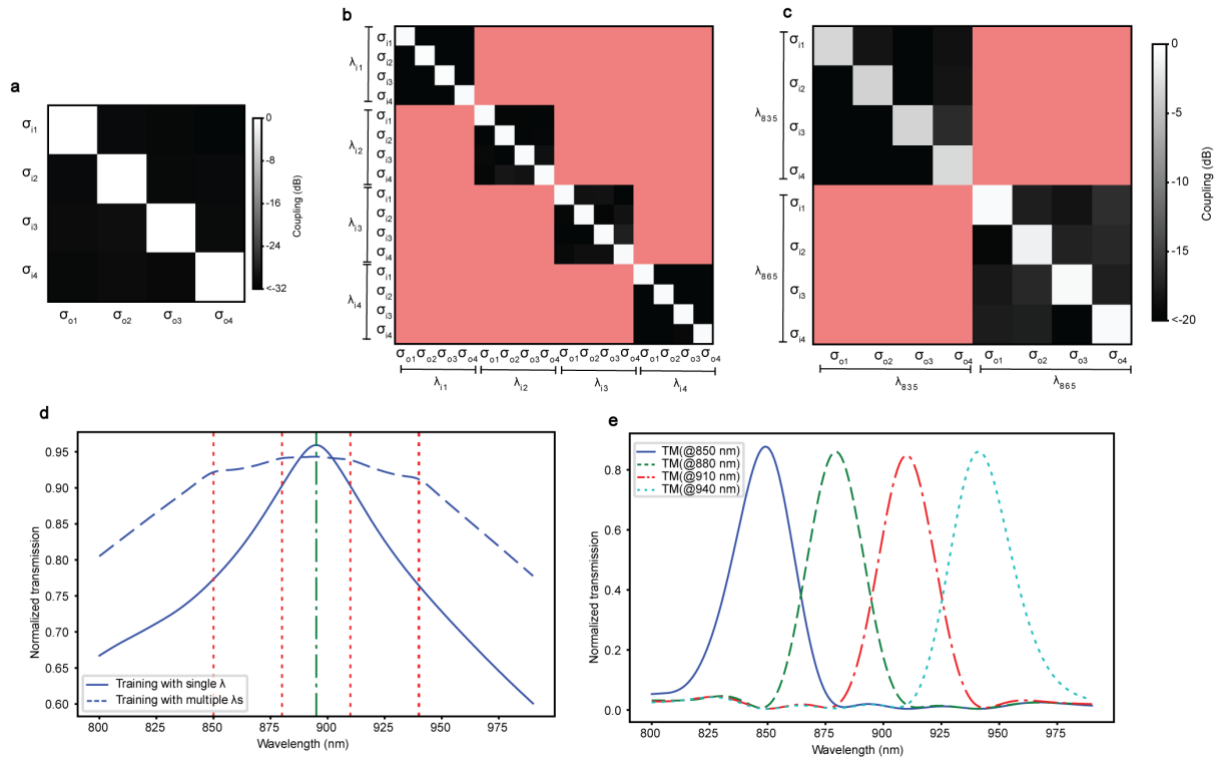


Figure 3: Efficiency and crosstalk results of MORS for broadband and wavelength-selective operation. The reordered transmission matrix (TM) is employed, where diagonal elements illustrate the power coupling from the n^{th} spatial input port σ_{in} to the n^{th} spatial output port σ_{on} per wavelength. Off-diagonal elements are crosstalk between target and other ports. a) Simulated TM for a single wavelength with four spatial ports is depicted, providing insights into the connectivity map. b) Combined simulated TMs for four different wavelengths are presented, showcasing distinct connectivity maps for each wavelength channel, all share spatial ports. c) Experimentally measured TMs for two wavelength channels (835nm, 865nm) are included, demonstrating the practical application of MORS. d) Average optical power

transmission for broadband TM application (covering the same TM over a 100nm range) is illustrated, we present power transmissions for both single and multiple wavelength training cases. e) Power transmission of four different wavelengths is shown while each wavelength has different connectivity map.

Discussion

Our study outlines the application of MORS, which leverages free space diffraction principles in combination with programmable spatial light modulation. Notably, this approach deviates from conventional methods that often rely on single paths. Instead, MORS introduces a novel optical path reconfiguration by employing spatial light modulation across multiple planes, thereby inherently incorporating multicasting capabilities. Promising scaling trends from numerical studies are substantiated by experimental validation. It is noted that free-space techniques inherently present efficient throughput, a key advantage over integrated solutions where factors like waveguide loss and coupling losses can impact scaling. Moreover, the ability to operate on the wavefront facilitates optimization with respect to the space-bandwidth product of output fibers, an ongoing challenge for MEMS-based systems as they must be very accurate in the corresponding angle for the output fiber. This becomes practically impossible without live feedback [4] as the beam size gets larger, which restricts the bandwidth immensely resulting in micro-radian level accuracy requirement. This is the fundamental reason why those systems cannot overcome a certain insertion loss, which is reported to be around 3 dB in various studies [23]. Moreover, LCoS technology provides sufficient switching speed (up to 1 ms considering commercially available devices), particularly for the switches that are placed at higher hierarchical levels in the networking fabric [4]. This switching speed surpasses that of some mechanical-actuation-based systems currently in use [23].

Comparable architectures for multiplexing/demultiplexing fiber modes have been documented in the literature, showcasing versatility across varied mode domains and input/output grid geometries [14, 24, 25]. With MORS, the efficiency of multicasting remains consistent, offering a potential resolution to longstanding challenges in conventional optical systems. Our research also demonstrates the capability to manage both space and spectrum in the interconnect, signaling a potential shift in

optical interconnect approaches. This not only enhances the reconfigurability of optical paths but also broadens the spectrum of wavelengths and spatial inputs that can be accommodated.

To conclude, MORS offers a new perspective in network design, potentially bridging the efficiency gap in multicasting present in today's optical interconnect technologies with additional flexibility by possessing space-wavelength granularity.

Methods

For our experiments, a continuous wave Solstis M2 laser was employed. The selected mirror, measuring 11.6 mm in width, accommodates the four reflections. To channel the beam to the SLM, 4F imaging was applied, relaying the beam that was reflected off a digital micromirror device (DMD). This DMD acts to simulate the input grid by activating specific sub-regions. For the modulation layers, we designated patches of 280 by 280 pixels on the SLM. The SLM used in our arrangement has a pixel pitch of $\Lambda=9.2\text{ }\mu\text{m}$. To establish the multi-bounce cavity, we integrated a Spatial Light Modulator (SLM) and set the mirror 17.1 mm away from the SLM screen. This spacing ensures that the diffraction from one layer's corner pixel can reach the opposite corner of the subsequent layer, facilitating comprehensive pixel connectivity. The setup facilitates four mirror reflections of the input beam. Following the fourth reflection, the beam is imaged, with the resultant output intensity captured by a CMOS camera.

In numerical scaling studies, we employed six diffractive layers. Layer width is set to 640 pixels for multicast case. For wavelength selective numerical experiments, we also used six diffractive layers having layer width of 360. Layer to layer distance is set to four millimeters for both cases. The details about the training method can be found in [22].

References

- [1] McKeown, N., Anderson, T., Balakrishnan, H., Parulkar, G., Peterson, L., Rexford, J., Shenker, S., & Turner, J. (2008). OpenFlow: enabling innovation in campus networks. *ACM SIGCOMM computer communication review*, 38(2), 69-74.

- [2] Farrington, N., Porter, G., Radhakrishnan, S., Bazzaz, H. H., Subramanya, V., Fainman, Y., Papen, G., & Vahdat, A. (2010, August). Helios: a hybrid electrical/optical switch architecture for modular data centers. In Proceedings of the ACM SIGCOMM 2010 Conference (pp. 339-350).
- [3] Poutievski, L., Mashayekhi, O., Ong, J., Singh, A., Tariq, M., Wang, R., Zhang, J., Beauregard, V., Conner, P., Gribble, S., Kapoor, R., Kratzer, S., Li, N., Liu, H., Nagaraj, K., Ornstein, J., Sawhney, S., Urata, R., Viciano, L., Yasamura, K., Zhang, S., Zhou, J., & Vahdat, A. (2022, August). Jupiter evolving: transforming google's datacenter network via optical circuit switches and software-defined networking. In Proceedings of the ACM SIGCOMM 2022 Conference (pp. 66-85).
- [4] Urata, R., Liu, H., Yasumura, K., Mao, E., Berger, J., Zhou, X., Lam, C., Bannon, R., Hutchinson, D., Nelson, D., Poutievski, L., Singh, A., Ong, J., & Vahdat, A. (2022). Mission Apollo: Landing optical circuit switching at datacenter scale. arXiv preprint arXiv:2208.10041.
- [5] Shahbaz, M., Suresh, L., Rexford, J., Feamster, N., Rottenstreich, O., & Hira, M. (2019). Elmo: Source routed multicast for public clouds. In Proceedings of the ACM Special Interest Group on Data Communication (pp. 458-471).
- [6] Xia, Y., Ng, T. E., & Sun, X. S. (2015, April). Blast: Accelerating high-performance data analytics applications by optical multicast. In 2015 IEEE Conference on Computer Communications (INFOCOM) (pp. 1930-1938). IEEE.
- [7] Das, S., Rahbar, A., Wu, X. C., Wang, Z., Wang, W., Chen, A., & Ng, T. E. (2022). Shufflecast: An optical, data-rate agnostic and low-power multicast architecture for next-generation compute clusters. IEEE/ACM Transactions on Networking.
- [8] Samadi, P., Gupta, V., Xu, J., Wang, H., Zussman, G., & Bergman, K. (2015). Optical multicast system for data center networks. Optics express, 23(17), 22162-22180.
- [9] Barry, L. P., Wang, J., McArdle, C., & Kilper, D. (2018). Optical switching in datacenters: architectures based on optical circuit switching. *Optical switching in next generation data centers*, 23-44.
- [10] Stepanovsky, M. (2019). A comparative review of MEMS-based optical cross-connects for all-optical networks from the past to the present day. IEEE Communications Surveys & Tutorials, 21(3), 2928-2946.
- [11] D. M. Marom, Y. Miyamoto, D. T. Neilson and I. Tomkos, "Optical Switching in Future Fiber-Optic Networks Utilizing Spectral and Spatial Degrees of Freedom," in Proceedings of the IEEE, vol. 110, no. 11, pp. 1835-1852, Nov. 2022, doi: 10.1109/JPROC.2022.3207576.
- [12] Marom, D. M., Colbourne, P. D., D'errico, A., Fontaine, N. K., Ikuma, Y., Proietti, R., ... & Tomkos, I. (2017). Survey of photonic switching architectures and technologies in support of spatially and spectrally flexible optical networking. Journal of Optical Communications and Networking, 9(1), 1-26.

- [13] Li, J., Gan, T., Bai, B., Luo, Y., Jarrahi, M., & Ozcan, A. (2023). Massively parallel universal linear transformations using a wavelength-multiplexed diffractive optical network. *Advanced Photonics*, 5(1), 016003.
- [14] N. U. Dinc, J. Lim, E. Kakkava, C. Moser, and D. Psaltis, "Computer generated optical volume elements by additive manufacturing," *Nanophotonics*, vol. 9, no. 13, pp. 4173–4181, Jun. 2020, doi: 10.1515/nanoph-2020-0196.
- [15] Xu, Y., Huang, J., Yang, L. et al. Inverse-designed ultra-compact high efficiency and low crosstalk optical interconnect based on waveguide crossing and wavelength demultiplexer. *Sci Rep* 11, 12842 (2021). <https://doi.org/10.1038/s41598-021-92038-w>
- [16] Lee, H., Gu, X. G., & Psaltis, D. (1989). Volume holographic interconnections with maximal capacity and minimal cross talk. *Journal of applied physics*, 65(6), 2191-2194.
- [17] Dinc, N. U., Moser, C., & Psaltis, D. (2024). Volume holograms with linear diffraction efficiency relation by $(3+1)$ D printing. *Optics Letters*, 49(2), 322-325.
- [18] U. S. Kamilov et al., "Learning approach to optical tomography," *Optica*, vol. 2, no. 6, p. 517, Jun. 2015, doi: 10.1364/OPTICA.2.000517.
- [19] L. Tian and L. Waller, "3D intensity and phase imaging from light field measurements in an LED array micro-scope," *Optica*, vol. 2, no. 2, p. 104, Feb. 2015, doi: 10.1364/OPTICA.2.000104.
- [20] X. Lin et al., "All-optical machine learning using diffractive deep neural networks," *Science*, vol. 361, no. 6406, pp. 1004–1008, Sep. 2018, doi: 10.1126/science.aat8084.
- [21] J. Lim, A. B. Ayoub, E. E. Antoine, and D. Psaltis, "High-fidelity optical diffraction tomography of multiple scattering samples," *Light Sci Appl*, vol. 8, no. 1, p. 82, Dec. 2019, doi: 10.1038/s41377-019-0195-1.
- [22] Yildirim, M., Dinc, N. U., Oguz, I., Psaltis, D., & Moser, C. (2023). Nonlinear Processing with Linear Optics. *arXiv preprint arXiv:2307.08533*.
- [23] Sato, Ken-ichi. "Optical switching will innovate intra data center networks [Invited Tutorial]." *Journal of Optical Communications and Networking* 16, no. 1 (2023): A1-A23.
- [24] N. K. Fontaine, R. Ryf, H. Chen, D. T. Neilson, K. Kim, and J. Carpenter, "Laguerre–Gaussian mode sorter," *Nature Commun.*, vol. 10, no. 1, pp. 1–7, Dec. 2019.
- [25] Labroille, G., Denolle, B., Jian, P., Genevaux, P., Treps, N., & Morizur, J. F. (2014). Efficient and mode selective spatial mode multiplexer based on multi-plane light conversion. *Optics express*, 22(13), 15599-15607.